

# Two-dimensional electrical imaging for detection of hydrocarbon contaminants

A. Godio<sup>1\*</sup> and M. Naldi<sup>2</sup>

<sup>1</sup> Politecnico di Torino, Italy

<sup>2</sup> Techga Servizi S.r.l – Torino, Italy

Received September 2001, revision accepted March 2003

## ABSTRACT

The effects of a long-term diesel oil pollution due to leakage from buried tanks have been investigated using electrical resistivity tomography. The reliability of 2D electrical resistivity imaging of the subsoil was assessed using a numerical modelling approach that simulated the different behaviour of the contaminated zone. The effects of inversion parameters, such as the damping factor and smoothing matrix, have been studied in order to evaluate the optimal parameters to process real data.

The results of the field test indicated that highly conductive anomalies can be related to the biological degradation of hydrocarbons: geochemical analysis performed on several groundwater samples confirmed the presence of biodegradation activity. Chemical analysis pointed out an anomalous concentration of iron and manganese cations dissolved in the groundwater. Very low values of resistivity can be associated with a marked modification of the cation exchange capacity of the soil mixture due to degradation of these hydrocarbons. Chemical and physical interactions due to hydrocarbon pollution affect the electrical properties of soils and groundwater.

## INTRODUCTION

In the site characterization of contaminated land, the costs and environmental impact of drilling numerous boreholes make it desirable to develop less costly and more environmentally friendly techniques. Many non-invasive geophysical methods have recently been applied to reduce the adverse impact of drilling on the environment and to lower the costs of site characterization, monitoring and remediation. Electrical Resistivity Tomography (ERT) is a geophysical technique that has been successfully applied to monitor contaminated groundwater (Barker 1996). We describe its use in investigating leachate plumes caused by leakage from underground storage tanks that contain hydrocarbons.

Geoelectrical and electromagnetic methods have been widely employed in environmental geophysics over the last 10 years: high-resolution electrical methods have been developed to detect and monitor leachate in landfills, to map the waste distribution in controlled and abandoned landfills and to detect organic and inorganic contaminants

in soils and groundwater. There is an increasing interest in the use of high-resolution resistivity surveys to investigate contaminants, particularly concerning the plume migration.

The behaviour of the electrical resistivity of contaminants, with respect to the host environment, depends on several factors, such as the host lithology, the soil moisture and the solubility of the contaminants in the groundwater. For organic contaminants that are not miscible with water, such as diesel fuel and gasoline, the complexity of chemico-physical reactions with the host environment makes it unrealistic to determine a typical range of resistivity which could enable differentiation of the plume from its surroundings. These phenomena can significantly affect the electrical and electromagnetic properties of the soil and groundwater and make the clear and unambiguous detection of contaminants very difficult. Many papers have reported seemingly contradictory results on the electrical and electromagnetic response of different contamination events. Mazac *et al.* (1990) pointed out the shortcomings of surface electrical methods in the detection of thin layers of the free hydrocarbon phase above the water table, although borehole investigations and tomographic data processing can overcome this

---

\*alberto.godio@polito.it

problem under some conditions (Morelli and LaBrecque 1996; Godio and Morelli 1998). The electromagnetic response at radio frequency is complicated by the possible effects of the vapour phase and by the different behaviour of the contamination in the vadose zone and underlying groundwater zone (Benson 1995). Geophysical methods are unable to detect some contaminants at the low concentrations of parts per billion that are of regulatory concern, although toluene can sometimes be detected with the complex resistivity technique, due to its chemical reactions with clay minerals. Complex electrical tomography has been reported to be successful in the detection of diesel pollution in the vadose zone (Kemna *et al.* 1999) even though great care must be taken to avoid electromagnetic coupling effects on the experimental data. Perhaps, the best way of identifying contaminants in small concentrations is by detecting their movement through repeated time-lapse geophysical measurements (Barker and Moore 1999).

Hydrocarbons usually show very high resistivity values, but the electrical behaviour of hydrocarbons in soil or in groundwater can be affected by biodegradation. This phenomenon usually leads to an increase in the conductivity of the aquifer (Atenkawa *et al.* 1998). This leads to remarkable variations in the dissolved ions in the fluid phase of the subsoil. For example, high concentrations of dissolved iron are associated with benzene biodegradation coupled to iron reduction. On the other hand, biodegradation of the benzene consumes sulphate and reduces the total amount of free sulphate ions. Contaminated soils and groundwater usually show very low resistivity values due to the imbalance of the sulphate reduction and the production of dissolved iron.

In this complex scenario, our experience has shown that pollution caused by LNAPL (light non-aqueous phase liquid) hydrocarbons (diesel oil) can be investigated using electrical tomography. In a study of an industrial site where hydrocarbon contamination was thought to be a problem, several electrical imagings were carried out to verify the possible leakage of diesel oil from three underground storage tanks into the subsoil. The study involved geochemical and geophysical investigations of the industrial site.

## GEOLOGY OF THE SITE AND DATA ACQUISITION

The investigated site is located in the southern part of the alluvial plain of Turin (Italy). The upper part of the sedimentary sequence is built up of recent alluvial deposits (silty and sandy gravel with some rare clayey lenses) which overlie an older fluvio-glacial sequence made up of silt and clay deposits with gravel. The phreatic water table is quite shallow, located at a depth of about 5 m, and the flow direction is to the south-east.

The location of the ERT profiles were planned in order to cross the groundwater flow direction in the industrial area, taking the available space inside the industrial site into account. Measurements were acquired by a Syscal Jr instrument connected to lines of 48 electrodes, using the Wenner configuration. A small electrode spacing of 1 m was adopted, in order to be able to provide considerable detail of any plumes related to leakage from the underground tanks. The locations of some lines, close to the diesel oil leaking source, are shown in Fig. 1.

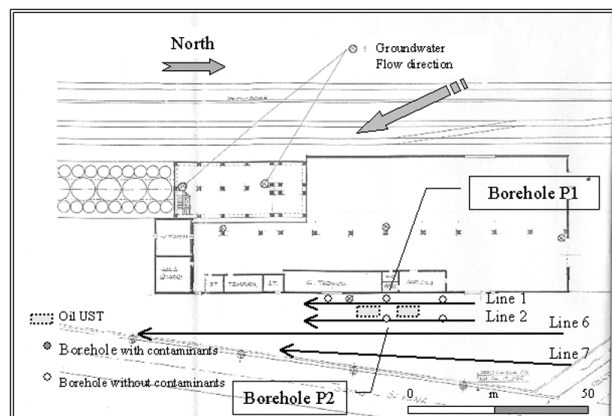


FIGURE 1  
Plan view of the site with location of the ERT lines.

It is well known that the Wenner array is relatively sensitive to vertical changes of resistivity below the centre of the array, but is not so sensitive in delineating narrow vertical structures. On the other hand, good quality data can be acquired in comparison with other conventional arrays in noisy areas. Therefore, the choice of the array was conditioned by the compromise between spatial resolution and the need to acquire good quality data in an area with potentially high background noise due to the presence of the asphalt coverage and man-made structures.

## CONSIDERATIONS ON THE ELECTRICAL RESPONSE OF HYDROCARBON-CONTAMINATED SOIL

Different physico-chemical behaviour can be determined from the interference of hydrocarbon pollutants and the subsoil. It is useful to simplify the electrical response of the hydrocarbon pollution of the subsoil using two different resistivity models. In the first case, the contaminant plume provides a very high conductive zone in the saturated and vadose zone, because of the presence of strong natural bioactivity. The second reference model considers a thin contaminated layer above the water table, simulated by a highly resistive layer (free hydrocarbon phase).

TABLE 1 Anomalous concentrations of contaminants in the groundwater

Particle	P1 ppb	P2 ppb	P3 ppb	P4 ppb	PA ppb
Iron	76	160	<b>260</b>	89	53
Manganese	<b>175</b>	541	<b>786</b>	<b>88</b>	37,2
Zinc	1,01	3,36	2,49	1,28	<b>878</b>
Dissolved hydrocarbons	< 3	<b>35,4</b>	< 3	< 3	< 3

The electrical conductivity of the groundwater can be approximated by summing up the contribution of the different ions multiplied by their mobility, according to the relationship:

$$\sigma = 96.5 \sum C_i m_i \quad [\text{S/m}], \quad (1)$$

where  $C_i$  is the number of gram equivalent weights of the  $i$ th ion per cubic metre of water and  $m_i$  is the mobility of the  $i$ th ion [ $\text{m}^2/\text{s V}$ ]. In the experimental test, the chemical analyses, performed on the specimens of groundwater, have indicated the presence of anomalous concentrations of iron, manganese and also zinc, for the PA borehole (Table 1). The increase in ions dispersed in the groundwater, caused by biological activity, therefore, does not seem to justify the significant changes in resistivity that are highlighted by the electrical tomography. This fact was fully analysed, according to the empirical relationship suggested by Waxman and Thomas (1974), where the specific resistivity of shale and sands depends on the cation exchange capacity (CEC), as given by the following formula:

$$\rho_0 = F \rho_w (1 + B Q_v \rho_w)^{-1}, \quad (2)$$

where  $\rho_0$  is the bulk resistivity,  $\rho_w$  the fluid resistivity,  $F$  is the formation factor, and the parameter  $B$  describes the slight interface conductivity dependence on the ion content, given by

$$B = 3.83 [1 - 0.83 \exp(-0.5/\rho_w)], \quad (3)$$

The parameter  $Q_v$  is related to the cation exchange capacity (CEC), according to

$$Q_v = \frac{1 - \phi}{\phi} \frac{d_s}{100} \text{CEC}, \quad (4)$$

where  $d_s$  is the grain soil density ( $\text{g/cm}^3$ ) and  $\phi$  is the porosity, CEC is given in milliequivalents per 100 g of soil matrix. The effects of CEC on the resistivity of the soil is shown in Fig. 2.

In the site experiment, it was possible to neglect the

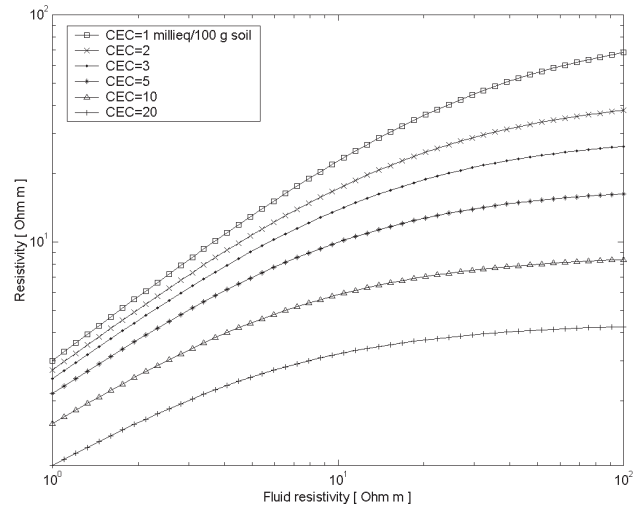


FIGURE 2

Resistivity response versus fluid resistivity for different CEC values of the soil.

effect of the double layer on the interface conductivity of clay because of the absence of clay minerals in the soil skeleton; the soil consists mainly of sandy material. On the other hand, a high CEC can be related to the organic matter that is present and which is enhanced by the biological activity in the contaminated soil.

The hydrocarbon contamination, trapped around the soil grains, and the biodegradation activity lead to:

- a decrease in the effective porosity of the pore water conductivity and an increase in the CEC of the organic matter of the soil; these effects cause an increase in the value of the  $Q_v$  parameter;
- a decrease in the fluid conductivity  $r_w$  as a consequence of the increasing ion content, which accounts for the increase of the  $B$  value that appears in formula (3);
- and finally, the increase in  $Q_v$  and  $B$  values and the decrease in the fluid conductivity lead to the decrease in the resistivity according to formula (2), which is only partially balanced by the variations in the formation factor value, due to the decrease of the interconnected porosity.

The influence of different factors on the inversion procedure was analysed to verify the reliability of the electrical resistivity images. In particular, we wanted to analyse the influence of the presence of a thick layer that was characterized by high resistivity values (the asphalt layer) and the effect of abrupt changes in resistivity between the uncontaminated and the contaminated soil and the groundwater. The accuracy of our data is better than 3%; bad measurements with a noise level higher than 3% were eliminated (about 5% of the data points was excluded). The effects of inversion parameters on the final results were also analysed. The standard smoothness-constrained least-squares method

is based on the solution of the following data set of equations (Loke 1995):

$$\Delta \mathbf{p} = (\mathbf{J}^T \mathbf{J} + \lambda \mathbf{C}^T \mathbf{C})^{-1} \mathbf{J}^T \Delta \mathbf{d}, \quad (5)$$

where  $\lambda$  is the Lagrangian multiplier or damping factor, used to stabilize the solution of the ill-posed tomographic problem,  $\mathbf{J}$  is the partial derivative matrix of the potential function with respect to the model resistivity parameter,  $\mathbf{C}$  is the smoothing matrix; vector  $\Delta \mathbf{p}$  is the perturbation of the model parameters for each iteration and  $\Delta \mathbf{d}$  is the vector that contains the differences between the observed and computed apparent resistivity values. The smoothing matrix  $\mathbf{C}$  enables constraints to be introduced on to the vertical or horizontal elongation of the structures.

The effects of the tomographic inversion reliability were explored using a numerical simulation approach (Sasaki 1992) that considered the effect of the damping factor and the array configuration on the quality of the inversion results. The damping factor leads to a stabilization of the solution but produces a smoothed resistivity model: a smoothed section provides for a realistic solution where a gradual change in contamination or a different effect of the natural attenuation can be expected. On the other hand, a low damping factor should offer a better interpretable section in the case of high contrast between the free phase of hydrocarbon and the uncontaminated groundwater. A near-surface highly resistive layer was considered to approximate the asphalt coverage; the uncontaminated aquifer was characterized by a resistivity of 50  $\Omega\text{m}$  and the contaminated zone was considered to be very conductive (2  $\Omega\text{m}$ ), according to the above theoretical formulation.

The model and the pseudosection of apparent resistivity, as obtained from the finite-difference forward computation (Dey and Morrison 1979), are shown in Fig. 3. A normally distributed noise of 5% was introduced into the synthetic data and the least-squares smoothness-constrained analysis was performed, according to relationship (5), using different values of damping factor to stabilize the solution. It was verified that a damping factor in the range of 0.01 to 0.25 does not affect the resolution of the inverted section to any great extent and provides very similar final models with an rms misfit of about 5%. The conductive anomaly appears to be spatially well resolved, as is the resistivity contrast between the contaminated and clean soil (Fig. 4).

In the second model, a free phase hydrocarbon is assumed to be above the aquifer without any relevant mineralization effects (biodegradation). In such a context, the shallow aquifer is contaminated by a non-miscible hydrocarbon phase and by a small amount of the total volume of hydrocarbon dissolved in groundwater. Only the LNAPL (light non-aqueous phase liquid) contamination was considered as the free phase hydrocarbon; this moves horizontally

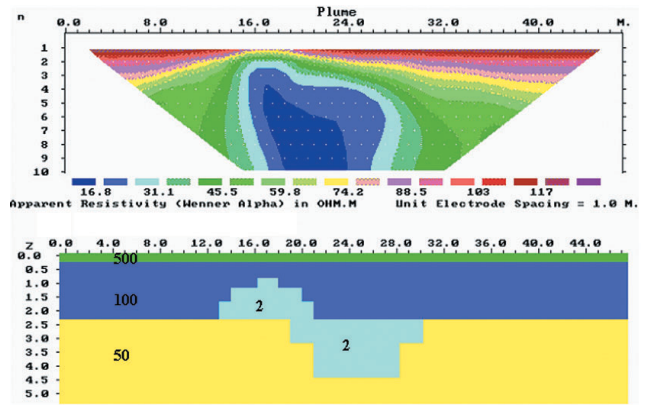


FIGURE 3 Model (bottom) and synthetic resistivity (top) for a Wenner array - 48 electrodes, assuming that the hydrocarbon contamination is characterized by a conductive response (resistivity values in  $\Omega\text{m}$ ).

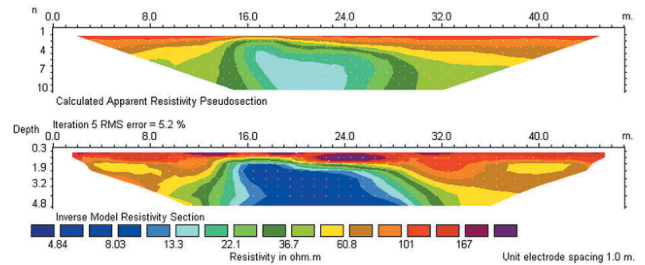


FIGURE 4 Inversion of synthetic resistivity data with 5% of normally distributed noise  $\lambda = 0.25-0.1$  and slow horizontal constraints for the model in Fig. 2.

above the water table, according to the hydrogeological condition of the area. The thickness of the free phase contaminant above the water table is less than a few centimetres.

The formulation proposed by Worthington (1976), and later discussed by Mazac *et al.* (1990), considers the resistivity response of the aquifer, fully saturated by uncontaminated groundwater, oil or a non-miscible mixture of these. The matrix resistivity value includes the influence of the oil-wetting or water-wetting phase in addition to the influence of the resistivity of the soil skeleton.

In a more general sense, the resistivity of the fluid phase includes the cation exchange capacity effects on the resistivity of the medium due to the interaction between the solid matrix and the mixture of the fluid phases. The aquifer resistivity ( $\rho_a$ ) depends on the soil matrix resistivity ( $\rho_m$ ) and the fluid resistivity ( $\rho_f$ ). It is expressed by the relationship (Mazac *et al.* 1990),

$$\rho_a = \frac{a \rho_m \rho_f^{2n}}{a \rho_w 10^{2n} + \rho_m (100\phi)^n}, \quad (6)$$

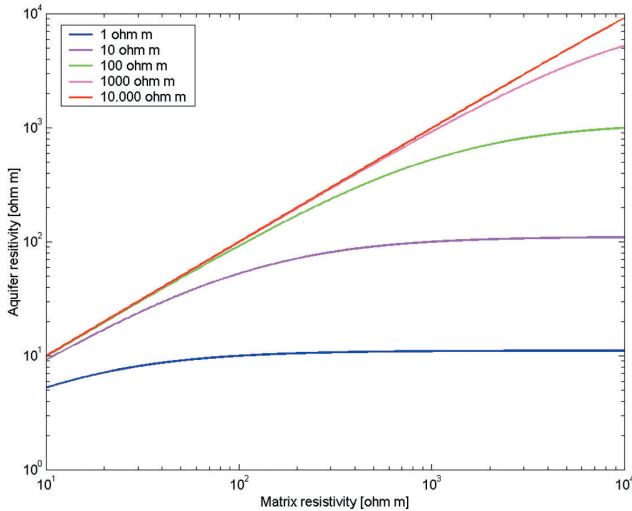


FIGURE 5  
Response of the fully saturated medium versus resistivity of the solid matrix for different values of fluid resistivity (resistivity values in  $\Omega\text{m}$ ).

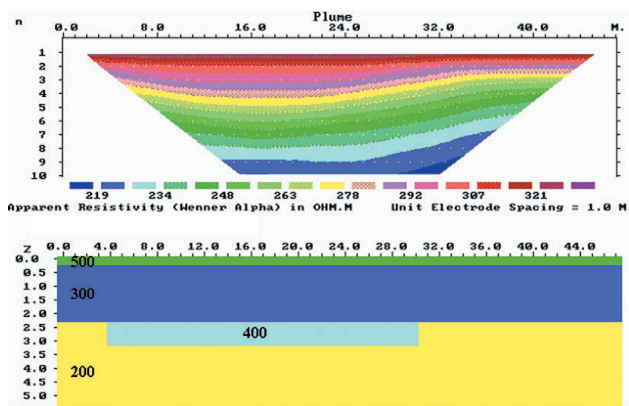


FIGURE 6  
Model (bottom) and synthetic resistivity data (top) for a Wenner array - 48 electrodes, assuming a free phase hydrocarbon contamination as a highly resistive layer on the water table (resistivity values in  $\Omega\text{m}$ ).

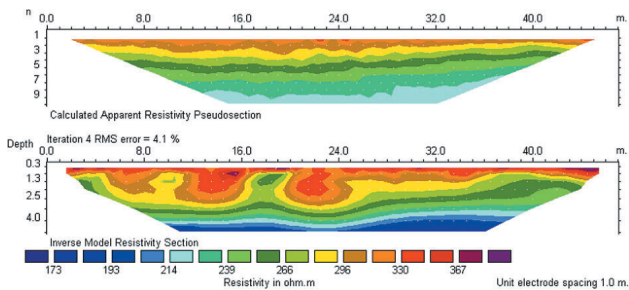


FIGURE 7  
Inversion of synthetic resistivity data with 5% of normally distributed noise  $\lambda = 0.25-0.1$  and low horizontal constraints for the model in Fig. 5.

where  $\phi$  is the soil porosity, while  $a$  and  $n$  are experimental parameters that depend on the textural and structural condition of the aquifer; the resistivity of the free phase of the hydrocarbon assumes values above  $10^6-10^8 \Omega\text{m}$ .

In the numerical model, the following parameters were inferred: the hydrocarbon free phase has a resistivity  $> 5 \cdot 10^5 \Omega\text{-m}$ , the uncontaminated groundwater has a resistivity of  $100 \Omega\text{-m}$  and the solid matrix has a resistivity between  $100$  and  $10\,000 \Omega\text{m}$ ; the soil porosity is  $0.3$ . As can be seen in Fig. 5, the difference in the resistivity of the contaminated layer compared to the uncontaminated soil is negligible for any matrix resistivity below  $200 \Omega\text{m}$ . A model was determined with a thick overburden layer (asphalt coverage at  $500 \Omega\text{m}$ ); the vadose zone was characterized by  $300 \Omega\text{m}$  and the lens of the LNAPL on the water table has a resistivity value of  $400 \Omega\text{m}$ , as estimated by equation (6) using  $a=1$  and  $n=2$ .

The model and the pseudosection of the apparent resistivity are shown in Fig. 6, as obtained through finite-difference forward computation. A normally distributed noise of 5% was introduced into the synthetic data and the least-squares smoothness-constraints inversion was performed.

The data inversion was carried out with different smoothing matrices and with different damping factors in the range between  $0.1$  and  $0.5$ . The selected simulation presented here (Fig. 7) considers a damping factor of  $0.25$  and constraints on the vertical changes of resistivity. It was noted that the resistive layer, which represents the hydrocarbon polluted zone, cannot be resolved in a medium resistive environment; only a small apparent depression of the water-table level is shown. Obviously, the resistivity value of the contaminated layer above the water table is not well resolved and the resistive structure is not horizontally elongated, as expected.

**EXPERIMENTAL RESULTS**

The data processing involved a tomographic inversion using a high damping factor and constraints on the vertical changes of resistivity. The results are depicted in four selected tomographic sections which are presented in Figs 8–11. The tomographic sections confirm the presence of a surface layer with high resistivity that covers the whole area, which refers to the asphalt coverage and the coarse gravel and sand level, as confirmed by a subsequent drilling.

The electrical response attributed to the diesel oil release (Figs 8 and 9) is indicated by the high conductivity anomaly in the central zone of the images. This result agrees with the suggestion that the oil release started several years before the investigation. The biodegradation occurred later on and modified the electrical response of the contaminated zone.

In order to verify the geophysical response, a series of

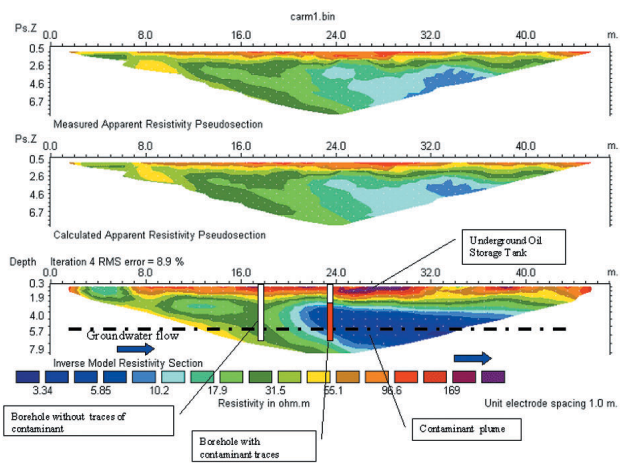


FIGURE 8 Electrical resistivity tomography – Line 1, showing positions of the boreholes.

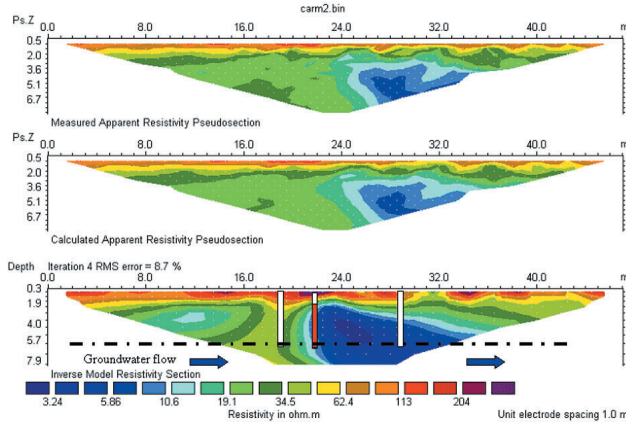


FIGURE 9 Electrical resistivity tomography – Line 2, showing positions of the boreholes.

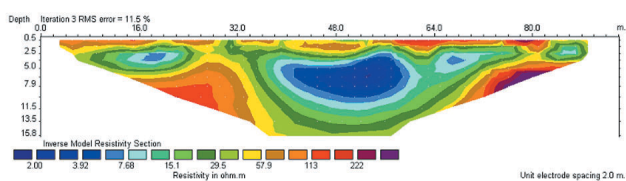


FIGURE 10 Electrical resistivity tomography – Line 6.

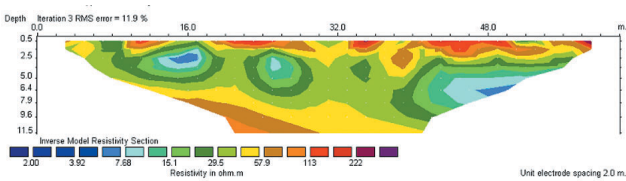


FIGURE 11 Electrical resistivity tomography – Line 7 in the uncontaminated zone.

boreholes was drilled on the site. Soil and water samples taken from the boreholes were analysed for contaminant detection. These have confirmed the detection of the plume defined by electrical tomography (Line 1 and Line 2). The two boreholes (P1 and P2) indicated traces of contaminants while no trace of pollution was found away from the main plume. The results of the chemical analyses have indicated a low concentration of hydrocarbons and an anomalous high content of iron (Table 1). The analysis of soil samples indicated the presence of TPH in a concentration of 200–250 mg/kg in the boreholes close to the tanks at a depth of 3–5 m below the surface; a low concentration of dissolved hydrocarbon was detected in the groundwater samples (35 mg/kg). The conductivity of uncontaminated groundwater is 350–400  $\mu\text{S}/\text{cm}$ ; values of 1000–1200  $\mu\text{S}/\text{cm}$  were measured for groundwater in the boreholes in the leaking zone. High values of dissolved oxygen were measured in the boreholes where high conductivity values were pointed out, whereas the measurements in boreholes outside the plume revealed low dissolved oxygen values. The anomalous concentration of iron and manganese values cannot be explained by direct contamination due to the industrial activity and confirmed a bacterial process involved in the degradation of hydrocarbons.

In the authors' opinion, only the effects of the mineralization of the diesel oil can be easily detected by electrical imaging, as this produces an extremely conductive response. On the other hand, the response of a thin layer of diesel oil lying above the groundwater table and not involved in the biodegradation process cannot be detected, as confirmed by the numerical simulation. When this is the case, electrical images can lead to a false evaluation of the subsoil volume affected by pollution.

**CONCLUSIONS**

The study pointed out the usefulness and the pitfalls of electrical tomography in the characterization of underground leakage of hydrocarbons. Experimental evidence, obtained from a joint geochemical and geophysical investigation approach, indicated that subsoil which has been saturated with diesel oil for a long period (> 20 years) exhibits an increased conductivity. It suggests that electrical tomography could be useful for monitoring the effects of induced biodegradation (bioremediation) through the repetition of the survey at different times, in order to observe any changes in the resistivity due to the increase of free ions resulting from hydrocarbon degradation. The strong conductivity anomaly, attributed to the hydrocarbon pollution zone, has been explained by increasing the organic activity and modification of the cation exchange capacity of the soil matrix. However, great care should be taken in the data pro-

cessing and interpretation in order to avoid misinterpretation of the effects of changes in soil moisture or pitfalls due to near-surface conductive bodies.

Numerical simulation permitted the effects of the inversion procedure on the resolution to be evaluated using a smoothing least-squares approach with a variable damping factor. It was verified that, in the case of long-term hydrocarbon pollution in aerobic conditions, when the effects of biodegradation activity can be estimated (mineralization of hydrocarbon, changes in CEC properties of the soils), the contaminated zone appears to be characterized as a highly conductive zone. In the present case, a smoothed solution using a high damping factor and smoothing matrix would be preferable.

Furthermore, under anaerobic conditions, where the biodegradation process is not so pronounced, it should be considered that the LNAPL, approximated by a resistive layer on the water table, can lead to misinterpretation of the ERT results.

#### ACKNOWLEDGEMENTS

We are greatly indebted to Ron Barker for his previous suggestions and for having encouraged us to improve the quality of the work. We thank A. Binley and A. Olayinka for their suggestions during the revision of the manuscript.

#### REFERENCES

- Atenkawa E.A., Sauck W.A. and Werkema Jr. D.D. 1998. Characterization of a complex refinery groundwater contamination plume using multiple geoelectric methods. Proceedings of the Symposium on the Application of Geophysics to Environmental and Engineering Problems, EEGS, Chicago, pp. 427–436.
- Barker R.D. 1996. Electrical imaging and its application in engineering investigations. In: *Modern Geophysics in Engineering Geology* (ed. D. McCann). Special publication of the Geological Society.
- Barker R.D. and Moore J. 1999. The application of time-lapse electrical tomography in groundwater studies. *The Leading Edge* **17**, 1454–1458.
- Benson A.K. 1995. Applications of ground penetrating radar in assessing some geological hazards: examples of groundwater contamination, faults, cavities. *Journal of Applied Geophysics* **33**, 177–193.
- Dey A. and Morrison H.F. 1979. Resistivity modelling for arbitrary shaped two-dimensional structures. *Geophysical Prospecting* **27**, 1020–1036.
- Godio A. and Morelli G. 1998. Mapping of complex hydrocarbons contaminant using geoelectric and electromagnetic methods. Proceedings of the 4th Meeting of Environmental and Engineering Geophysical Society (EEGS, European Section), Barcelona, Spain, pp. 19–22.
- Loke M.H. and Barker R.D. 1995. Least-squares deconvolution of apparent resistivity pseudosections. *Geophysics* **60**, 1682–1690.
- Kemna A., Dresen L. and Raekers E. 1999. Field applications of complex resistivity tomography. 69th SEG meeting, Houston, Texas, Expanded Abstracts, 331–334.
- Mazac O., Benes L., Landa I. and Maskova A. 1990. Determination of the extent of oil contamination in groundwater by geoelectrical methods. *Geotechnical and Environmental Geophysics: Environmental and Groundwater* **2**, 107–112.
- Morelli G. and LaBrecque D.J. 1996. Advances in ERT inverse modeling. *European Journal of Environmental and Engineering Geophysics* **1**, 171–186.
- Sasaki Y. 1992. Resolution of resistivity tomography inferred from numerical simulation. *Geophysical Prospecting* **40**, 453–463.
- Waxman M.H. and Thomas E.C. 1974. Electrical conductivity in shaly sands. *Journal of Petroleum Technology*, 213–225.
- Worthington P.F. 1976. Hydrogeophysical equivalence of water salinity, porosity and matrix conduction in arenaceous aquifers. *Ground Water* **14**, 224–232.

2<sup>ND</sup> HAND & NEW NEAR SURFACE GEOPHYSICAL EQUIPMENT

**RTCLARK.COM**  
Equipment @ Click

R.T. CLARK CO., INC. PO BOX 20957 OKLAHOMA CITY, OK 73156 USA TELE+1405-751-9696 FAX+1405-751-6711